Open Journal of Soil Science, 2023, 13, 371-390
https://www.scirp.org/journal/ojss
ISSN Online: 2162-5379
ISSN Print: 2162-5360

Re-Examining Field-Surveyed Variations in Elevation and Soil Properties with a 1-m Resolution LiDAR-Generated DEM

Kamille Lemieux, Paul A. Arp

Faculty of Forestry & Env. Management, University of New Brunswick, Fredericton, Canada
Email: arp1@unb.ca

How to cite this paper: Lemieux, K. and Arp, P.A. (2023) Re-Examining Field-Surveyed Variations in Elevation and Soil Properties with a 1-m Resolution LiDAR-Generated DEM. *Open Journal of Soil Science*, **13**, 371-390.
https://doi.org/10.4236/ojss.2023.139017

Received: August 22, 2023
Accepted: September 25, 2023
Published: September 28, 2023

Abstract

This article presents a 2017 LiDAR-DEM guided 1-m resolution examination of field-surveyed elevation and soil property variations (5 × 5 m spacings) conducted in 1977 across a hummocky New Brunswick field used for potato production. This examination revealed that the field incurred minor elevation differences were likely due to upslope erosion, as revealed through increasing Sand % and CF % with increasing elevation, and increasing Silt % along low-lying areas. Soil moisture, field capacity, permanent wilting and nitrate nitrogen (NO_3-N) also increased at downslope locations. Directly as well as indirectly, soil pH, ammonium nitrogen (NH_4-N), Caesium^{137} (Cs^{137}) and Mehlich-3 extracted Ca, Mg, K, Fe, Mn, Cu, and Zn were likewise affected by topographic location. Factor analyzing these variables led to: 1) a Soil Loss Factor that captured 24% of the textural variations; 2) a Soil-Cropping Factor accounting for 16% of the N, P, K, Ca, Mg, Mn variations; 3) a Soil Organic Matter (SOM) Factor relating 9% of the in-field variations for SOM, Fe, Zn, Cu to via organo-metal complexation and low NO_3-N retention. Many of the topographic variations increased or decreased with the metric DEM-projected depth-to-water index (DTW) index. This index was set to 0 along DEM-derived flow channels with minimum upslope flow-accumulation areas of 0.1, 0.25, 0.5, 1 or 4 ha. Among these, the DTW > 4 ha threshold was useful for reproducing the textural variations, while the DTW > 0.25 ha threshold assisted in capturing trends pertaining to moisture retention and elemental concentrations.

Keywords

Field-Elevation Survey, LiDAR 1-m DEM, Flow Channels, Depth-to-Water, Soil Properties, Factor Analysis

1. Introduction

The purpose of this study is to re-examine 1977-dated soil properties for a hummocky farm field near Hartland in New Brunswick (NB) as published by [1]. In this study, the elevations across the field were surveyed along a 5-m grid. Soil textural, morphological, and chemical properties were determined along a 25-m grid, and also along 5 × 5 m grid each at an uphill and a downhill location. The properties so analyzed refer to plough layer depth (Ap), soil texture, CF %, total soil organic carbon (TOC, *i.e.*, particulate combined with non-particulate organic matter), soil moisture content (MC), water retention at saturation point (SP), field capacity (FC) and permanent wilting point (PWP), pH, and soil extractable Ca, Mg, K, S, P, NO_3-N, NH_4-N, Fe, Mn, Cu, Zn, and Cs^{137}. This re-examination was facilitated through:

1) the availability of the 1-m resolution LiDAR DEM generated in 2017 [2], and

2) the metric cartographic depth-to-water delineation index DTW formulated in [3].

This index can be used approximate the areal extent of very poor to poor, imperfect, moderate, well and excessive soil drainage next to permanent open water bodies and channels as DTW varies from 0 to 10, 25, 50, 100 cm and more, respectively [3]. For forested areas, permanent flow channels generally require at least 4 ha of upslope flow-accumulation areas (FA) for end-of-summer surface flow [4]. Seasonally affected flow effects on channel-adjacent soil properties can also be analyzed by reducing the upslope FA requirement to, e.g., 1, 0.25 and 0.1 ha. The purpose for doing so refers to demonstrating how local uphill to downhill water flow and retention patterns affect measured within-field soil property variations.

2. Methods

2.1 Study Area

The field described by [1] is 175 × 425 m in width and length, and is approximately located 1 km one km east of Harland, NB (**Figure 1**; 46˚18'23''N 67˚30'41''W).

The geological surface deposit which is <2 m deep at this location refers to a sediment-derived loamy lodgment till with minor calcareous content. The soil that developed in this till is classified as an Orthic Humo-Ferric Podzol within the Carleton soil association. Cultivation - started 120 years ago - transformed the original mound-and-pitted forest soil underneath northern tolerant hardwoods to a smoothed surface with interrupted soil layer sequences. Across the surveyed field and beyond, intensified crop management since 1950 including potato cropping induced slope-dependent soil erosion coupled with soil re-deposition in depressions, at a rate of 22 to 53 tons/ha/year. Mean annual precipitation amounts to 1096 mm, with 796 mm from May to September. The mean monthly May to September temperature is 14.9˚C. The mean annual air temperature is 4.0˚C.

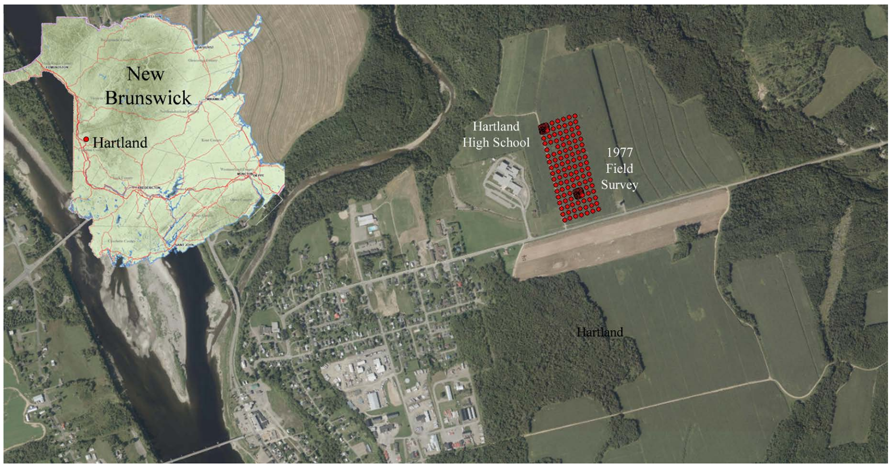

Figure 1. Locator map for the 1977 field survey in Harland, New Brunswick (46˚18'23"N, 67˚30'41"W).

2.2. Soil Analysis

The surface soil (primarily A-layer) was sampled (augured) and analyzed along the 25 m and 5 × 5 m grid for soil texture (hydrometer method without OM removal), CF content, and TOC concentration (combustion method using a Leco CNS-1000 analyzer). Also determined were the soil pH (1:1 water (H_2O)) and Mehlich-3 extractable Ca, Mg, K, S, P, Fe, Mn, Cu, and Zn [5]. The Mehlich-3 extract formulation is composed of 0.2 mole/liter (M) acetic acid (CH_3COOH), 0.25 M ammonium nitrate (NH_4NO_3), 0.015 M ammonium fluoride (NH_4F), 0.013 M nitric acid (HNO_3), and 0.001 M ethylenediaminetetraacetic acid (EDTA). Additional determinations involved:

1) 0 to 15 cm depth soil moisture levels on 11 July (MC1) and 27 August (MC2) 1997 using time domain reflectometry.

2) Calcium chloride ($CaCl_2$) extractable NH_4-N and NO_3-N.

3) Cs^{137}, using a Tennelec germanium crystal gamma radiation counter.

4) Soil saturation point (SP), field capacity (FC) and permanent wilting point (PWP).

All these determinations were done at and obtained from the Potato Research Centre of Agriculture and Agri-Food Canada in Fredericton, NB.

2.3. GIS Analysis

The GIS analysis was conducted with ArcMap using the 2017 LiDAR-generated 1-m DEM and Tarboton's D8 algorithm. Doing so generated the slope, filled, flow direction, flow accumulation, and flow channel rasters [6]. The latter were classified into flow channel networks with >4, 1, 0.5, 0.25, and 0.1 ha upslope flow accumulations for flow initiation. The slope and reclassified flow-channel raster were used to determine the cartographic cost-distance derived DTW (in m) so that the >4, >1, >0.5, >0.25, >0.1 ha DTW classifications would respectively represent DTW at the end of summer (>4 ha), following storm and rainfall events in summer (>1, >0.5, >0.25 ha), and at intense snowmelt times (>0.1 ha,

Figure 2). Also determined was the Topographic Position Index (TPI, [7] [8]) using mean 25-m annulus elevations as TPI = 0 m reference. The 1977 field-surveyed point data were subsequently supplemented with their corresponding 2017 DEM, DTW and TPI extracted values using the Multipoint Extraction tool.

2.4. Statistical Analysis

The combined and GIS generated point data were summarized using basic statistics followed by correlation and simple and multivariate linear regression analyses. The resulting correlation matrix was factor analyzed to reveal how the variables so summarized either relate or differ from each other by way of an explanatory three-factor pattern. The regression analyses were done to determine 1) how the field-surveyed and LiDAR-generated elevations vary in detail, and 2) how Sand %, Silt %, Clay %, CF %, SOM %, NO_3-N, NH_4-N, Soil Moisture Content, Field Capacity and Permanent Wilting Point are affected by topographic position in the form of the DTW variables as defined by their minimum upslope flow accumulation areas.

3. Results and Discussion

3.1. Data Summary

The data associated with the field-surveyed variables are presented in **Table 1**, together with their units, averages, standard deviations, and minimum and maximum values. The correlations for most of these variables are listed in **Table 2**.

3.2. Field-Surveyed (1977) versus LiDAR-Registered (2017) Elevations

The summary in **Table 1** reveals that the elevation changes from 1977 and 2017 were generally minor after accounting for the 84 m difference in resetting the 1977 to the 2017 zero-elevation reference level. Using the 2017 DEM as the only predictor variable for the 1977 elevation data produced a regression coefficient of <1 (*i.e.*, 0.941, **Table 3**, Analysis A). This means that the survey plot was somewhat flatter in 1977 than in 2017. Adding DTW > 4 ha and then Silt % to the regression analysis (**Table 3**, Analyses B and C):

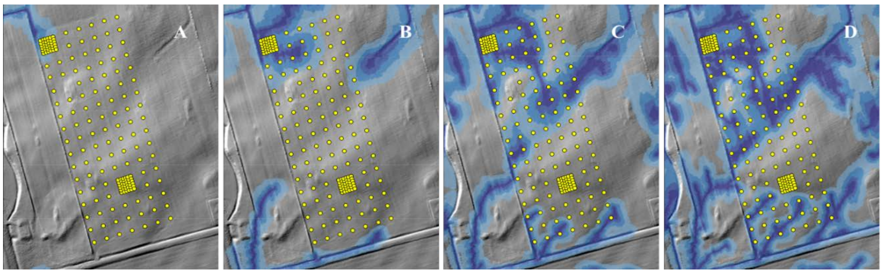

Figure 2. Survey grid and cartographic DTW associated from A to D, with the LiDAR-DEM derived flow channels with >4, 1, 0.25, and 0.1 ha upslope flow-accumulation areas, overlaid on the hillshaded DEM, respectively. DTW grades from <10 cm (dark blue) to 1 m (light blue) deep.

Table 1. Statistical summary of the field-surveyed variables with unit, mean, standard deviation, and maximum and minimum values.

Variable	Units	Mean	Std. Dev.	Min.	Max.
Ap	m	33.5	4.4	15	44.5
CF	cm	34.6	7.7	17.8	53.6
Sand	%	34.5	3.7	26.5	44
Silt	%	45.4	2.7	37.7	50.8
Clay	%	20.1	2.1	14.5	24.5
C	%	2.21	0.26	1.4	3.55
Ca	mg/kg	1503.5	239.2	1082.8	2252.2
Mg	mg/kg	188.3	25.4	129.3	260.3
K	mg/kg	176.7	40.7	101.6	281.6
P	mg/kg	327.4	53.4	186.2	470.3
S	mg/kg	81.6	17.7	36.7	141.9
Fe	mg/kg	311.2	34.6	219.2	402.3
Mn	mg/kg	39.7	13.2	19.1	120.4
Zn	mg/kg	3.49	1.15	1.87	10.22
Cu	mg/kg	5.19	1.1	3.1	8.72
Na	mg/kg	40.7	22.4	16.6	107.7
Cs^{137}	Bq/m^2	1690.5	487.5	665.6	3248.5
NO3-N	mg/kg	5.47	2.48	1.93	15.85
NH_4-N	mg/kg	0.48	0.19	0	1.01
pH-H_2O	-	5.4	0.25	4.84	6.08
Soil Moisture	%	17.4	1.8	13.7	25.7
2017 DEM	m	136.0	2.8	132	141.3
1977 DEM	m	51.9	2.6	47.6	57.2
2017 DEM - 1977 DEM	m	84.1	0.2	84.4	84.1
DTW > 0.1 ha	m	1.18	1.13	0	4.19
DTW > 0.25 ha	m	1.45	1.31	0	4.66
DTW > 0.5 ha	m	2.09	1.84	0	5.38
DTW > 1 ha	m	2.91	2.71	0	9.12
DTW > 4 ha	m	6.31	4.06	0	12.62
Slope	%	4.86	2.02	1.4	12.34
TPI	m	0.54	0.2	−0.48	0.53

DTW, Slope, TPI derived from 2017 DEM; Slope: focal 5 m circle mean; TPI = 2017 DEM - mean 25 m 2017 DEM annulus.

Table 2. Correlation matrix for most of the variables listed in **Table 1**. Significant regression coefficients (<−0.300 or >0.300) are highlighted in gray.

Correlation Matrix

Variables	Ap	CF	Sand	Silt	Clay	C	Ca	Mg	K	P	S	Fe	Mn	Zn	Na	Cs^{137}	NO_3-N	NH_4-N	pH	MC	DTW > 1 ha	DEM
Ap	1																					
CF	0.072	1																				
Sand	0.085	0.785	1																			
Silt	−0.004	−0.716	−0.843	1																		
Clay	−0.148	−0.498	−0.723	0.237	1																	
C	0.259	−0.194	−0.277	0.364	0.033	1																
Ca	−0.02	−0.182	−0.234	0.265	0.083	0.129	1															
Mg	−0.027	−0.094	−0.191	0.154	0.147	0.178	0.766	1														
K	0.018	0.368	0.206	−0.159	−0.167	−0.126	0.255	0.34	1													
P	−0.014	0.228	0.324	−0.204	−0.323	−0.145	0.423	0.387	0.354	1												
S	0.088	0.269	0.199	−0.204	−0.097	−0.096	0.095	0.124	0.4	0.263	1											
Fe	0.2	−0.194	−0.21	0.157	0.177	0.085	0.098	0.268	0.005	0.202	0.048	1										
Mn	−0.053	0.031	−0.022	−0.024	0.071	−0.231	0.493	0.489	0.229	0.546	0.174	0.45	1									
Zn	0.099	−0.04	−0.064	0.051	0.051	0.115	0.14	0.097	0.023	0.221	0.091	0.231	0.309	1								
Na	−0.099	0.284	0.272	−0.246	−0.175	0.079	−0.203	−0.246	−0.164	0.005	−0.207	−0.35	−0.153	0.075	1							
Cs^{137}	0.108	−0.417	−0.505	0.569	0.181	0.426	0.387	0.389	0.218	0.127	−0.058	0.273	0.188	0.087	−0.14	1						
NO_3-N	−0.148	−0.217	−0.316	0.276	0.215	−0.237	0.251	0.047	0.282	−0.052	0.214	−0.261	0.04	−0.059	−0.14	0.111	1					
NH_4-N	−0.111	−0.134	−0.083	0.089	0.036	−0.084	0.022	−0.163	−0.253	−0.032	−0.228	−0.233	−0.018	−0.033	0.353	−0.036	0.391	1				
pH	−0.044	0.024	−0.028	0.036	0.004	−0.116	0.617	0.473	0.347	0.21	−0.202	−0.04	0.348	0.009	−0.07	0.202	0.12	0.013	1			
MC1	−0.069	−0.264	−0.495	0.422	0.352	0.137	0.355	0.364	0.268	−0.085	0.112	0.184	0.154	0.015	−0.304	0.406	0.241	−0.097	0.268	1		
DTW > 1 ha	0.008	0.615	0.643	−0.545	−0.461	−0.12	0.001	0.029	0.074	0.349	−0.055	−0.06	0.219	0.036	0.394	−0.301	−0.381	0.101	0.111	−0.341	1	
1977 DEM	0.093	0.576	0.622	−0.568	−0.393	0.037	−0.477	−0.298	0.023	0.048	−0.037	−0.008	−0.144	0.035	0.503	−0.303	−0.544	−0.095	−0.231	−0.39	0.518	1

1) produced negative coefficients for these variables,

2) increased the R^2 values to 0.993 and 0.995,

3) rendered the 2017 DEM coefficient to become 1.010 and 1.002,

4) reduced the RMSE value of the residuals from 0.249 to 0.190 m.

The numerically flatter elevation profile across the 1977-surveyed field is in part related to 2017-DTW and 1977-Silt % adjustments. In detail, the 2017 DTW adjustments render the 1997 hilltop locations some smoother while the Silt % adjustments render the 1977 downhill locations somewhat deeper. Further adjustments towards a residual RMSE of 0.162 m were obtained by regressing the resulting 1977 DEM residuals (**Table 3**, Analysis D) against the 2017 Slope and 2017 TPI variables. The positive 2017 Slope coefficient suggests that some of the 1977 elevations were slightly higher along the steeper slopes than in 2017. The negative 2017 TPI coefficient implies that some of the knoll elevations were slightly less pronounced in 1977, and some of the depressed areas - where TPI < 0 m - were slightly more filled in 2017 than in 1977. **Figure 3** illustrates the extent to which some of the Analysis C residuals correspond to the underlying 2017 DEM derived Slope % and TPI rasters.

Table 3. Multivariate regressions(A, B, C) with the 2017 LiDAR DEM, DTW > 4 ha and 1977 Silt %as 1997 DEM predictor variables, followed by analyzing the resulting 1977 DEM residuals using the 2017 determined Slope and TPI variables (Table 1) as independent variables.

Variables	Mean	Std. Dev.	Std. Error	Count	Min.	Max.
1977 Elevation, m	51.9	2.61	0.19	190	47.6	57.2
2017 DEM, m	136	2.76	0.2	190	132	141.3
2017 DTW > 4 ha, m	6.3	4.1	29.5	190	0.47	12.6
1977 Silt %	45.4	2.65	0.19	190	37.7	50.8
1977 Elevation Analysis	**Regression Variables**		**Coeff.**	**Std. Error**	**t-Value**	**p-Value**
A: R^2 = 0.991; RMSE = 0.249 m	Intercept		−76.1	0.892	−85.3	<0.0001
	2017 DEM, m		0.941	0.007	143.5	<0.0001
B: R^2 = 0.990; RMSE = 0.213 m	Intercept		−84.9	1.302	−65.3	<0.0001
	2017 DEM, m		1.009	0.01	102.7	<0.0001
	2017 DTW > 4 ha, m		−0.056	0.007	−8.4	<0.0001
C: R^2 = 0.995; RMSE = 0.190 m	Intercept		−81.7	1.2	−65.6	<0.0001
	LiDAR DEM, m		1.002	0.009	113.7	<0.0001
	2017 DTW > 4 ha, m		−0.07	0.006	−11.2	<0.0001
	Silt, %		−0.047	0.007	−7.1	<0.0001
D: C Residuals: R^2 = 0.252; RMSE = 0.162 m	Intercept		−0.17	0.03	−5.6	<0.0001
	2017 Slope %, focal 5 m circle mean		0.039	0.006	6.6	<0.0001
	TPI: 2017 DEM - mean 25 m 2017 DEM annulus		−0.35	0.06	−5.7	<0.0001

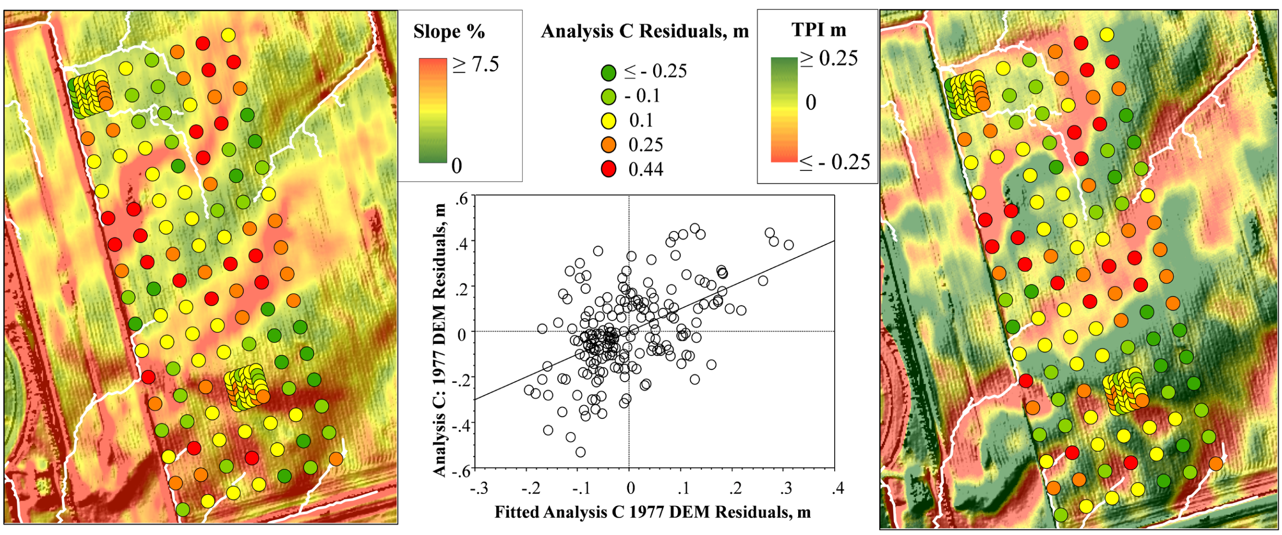

Figure 3. Analysis C (Table 3) residuals overlaid on Slope % (left) and TPI (right), together with the corresponding actual versus best-fitted scatterplot (center) and the 2017 DEM - derived flow channels with >0.25 ha upslope flow accumulation (white lines).

3.3. Regression Analyses: Sand, Silt, Clay and Coarse Fragment

Plotting Sand, Silt, Clay, and CF % versus DTW > 4 ha showed that Sand % increased but Silt and Clay % decreased with increasing DTW > 4 ha (**Figure 4**, left). The decreasing Clay % content with increasing DTW > 4 ha relates directly to the upland Si % loss, *i.e.*, clay displacement did not occur across the field. Hence, the higher lying areas were found to be coarser and sandier than the lower less well-drained areas. This would likely be due to natural and recurring cropping-induced upland-to-lowland silt-displacing soil erosion. In this regard, **Figure 4** (right) shows how surveyed CF % follows the underlying DTW > 4 ha pattern. This is further illustrated in **Figure 5** where the dotted 1977 CF % pattern is more closely aligned with the 2017 DEM derived DTW > 4 ha pattern than with the 2017 DEM pattern.

The very coarse (vc), coarse (c), and medium (m) sized fine (f) and very fine (vf) fractions of Sand also increased with increasing DTW> 4ha, but with the trend decreasing towards finer grain size such that vcSand > cSand > mSand and no discernable DTW > 4ha for vfSand (**Figure 6**, left). Testing to which extent the DEM-generated patterns for DTW > 4, > 1, > 0.25, and > 0.1 ha were related to the field-determined Silt % led to the regression results in **Figure 6** (right). The corresponding R^2 values change in the order:

DTW > 0.1 ha, R^2 = 0.286; DTW > 0.25 ha R^2 = 0.255; DTW > 1 ha, R^2 = 0.329; DTW > 4 ha, R^2 = 0.372.

This means that the field-assessed Silt % variations are best expressed by the slope-affected cost distance between each survey point and its closest > 4 ha down-stream location.

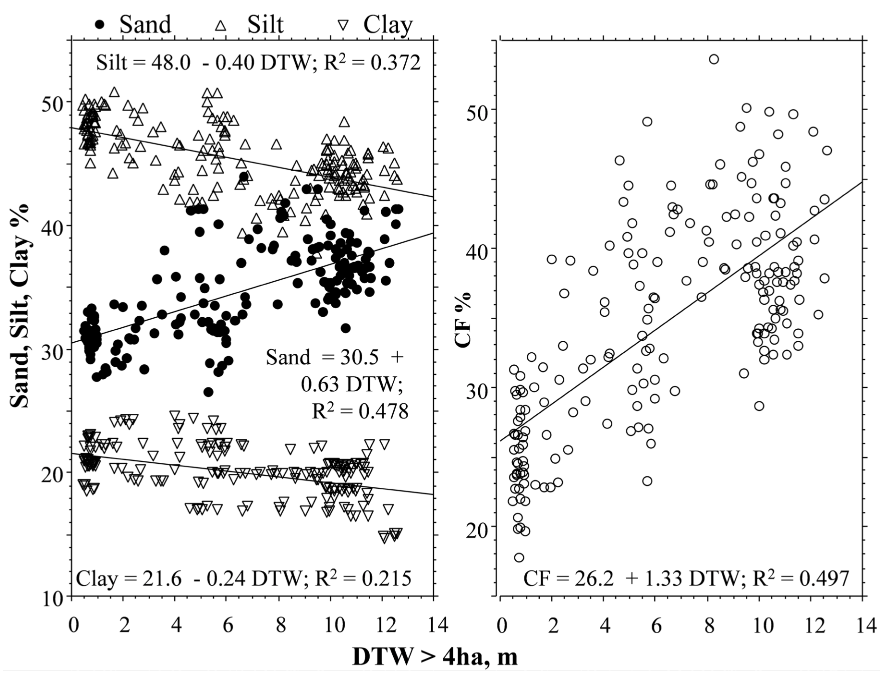

Figure 4. Sand, Silt, and Clay % (left) and CF % (right) versus DTW > 4 ha, all with regression equations.

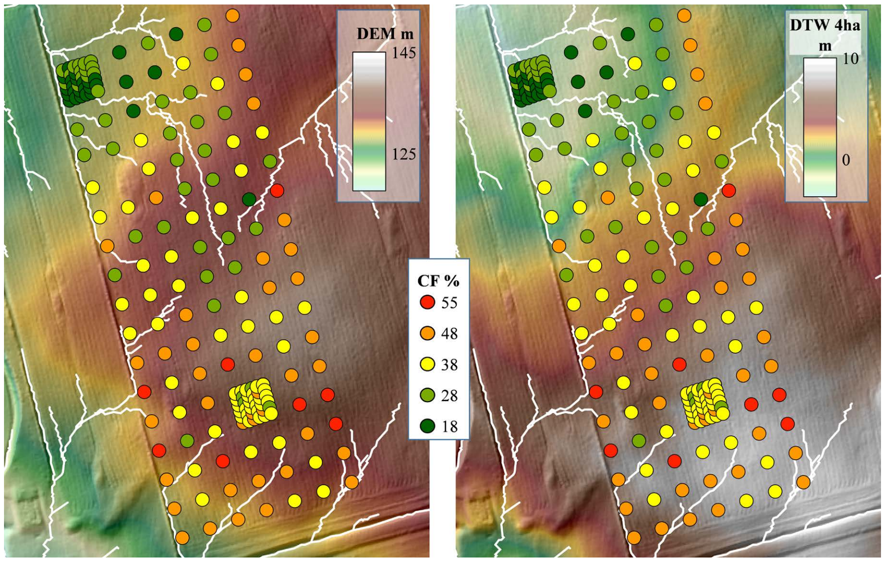

Figure 5. Surveyed CF % overlaid on the hillshaded 2017 DEM grid (left) and cartographic 2017 DTW > 4 ha grid (right). Also shown: 2017 DEM-derived flow channels with >0.1 ha upslope flow accumulation areas.

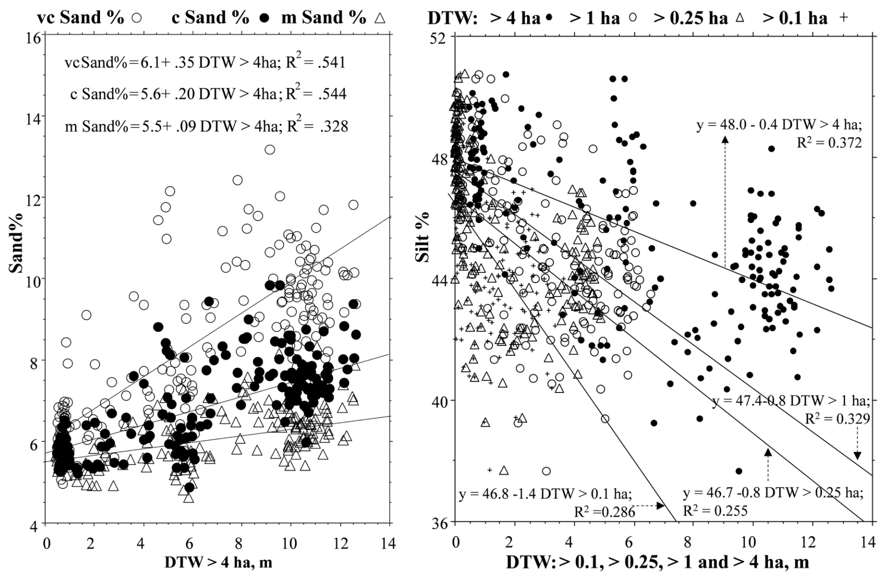

Figure 6. Left: decreasing trend from very coarse (vc) to coarse (c) and fine medium (m) Sand % fractions versus DTW > 4 ha upslope flow accumulation. Right: Silt % versus DTW (m) along the 2017 DEM derived flow channels with DTW > 4 ha, >1 ha, >0.25 ha and >0.1 ha upslope. All with regression equations.

3.4. Regression Analyses: Soil Moisture Content and Retention

Field capacity (FC %) and permanent wilting point (PWP %) increased significantly with decreasing DTW, with best results obtained using DTW > 0.25 ha as independent variable (**Figure 7**, left). In contrast, the soil saturation point was not so affected, *i.e.* SP % = 50.8 - 0.039 DTW > 0.25 ha (in m); R^2 = 0.001. In general, SP varies with soil bulk density, while FC and PWP increase with increasing soil organic matter and as soil textures become finer [9]. This suggests

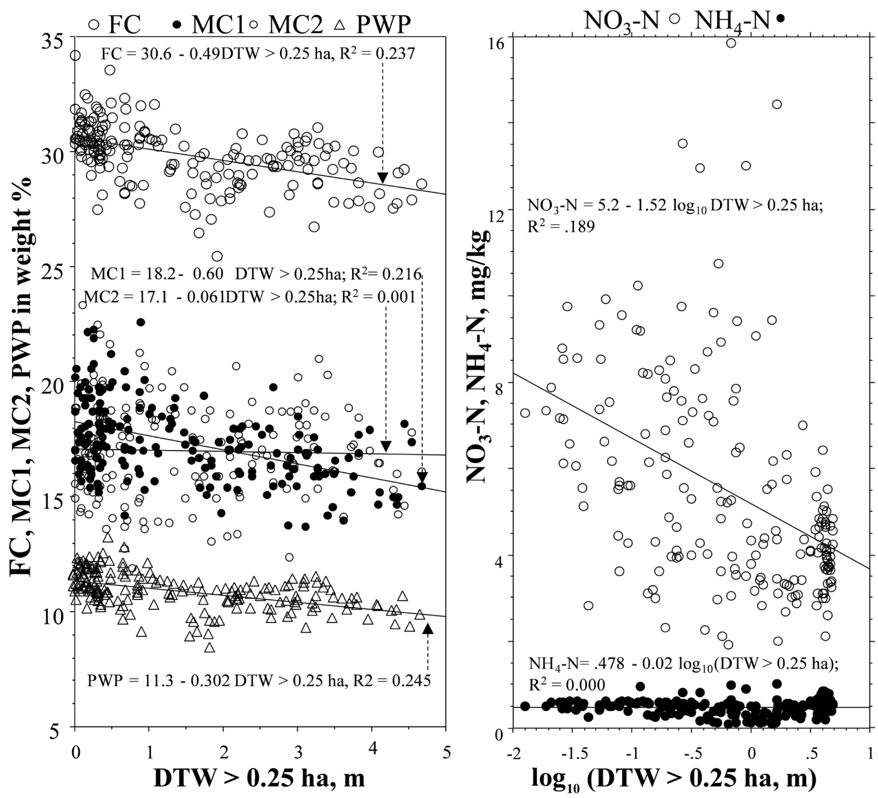

Figure 7. Left: Field Capacity (FC %), Soil Moisture (MC1 % and MC2 %), and Permanent Wilting Point (PWP %) versus DTW > 0.25 ha, in m. Right: NO_3-N and NH_4-N versus log_{10} (DTW > 0.25 ha, m).

that the bulk density of the soil was not affected by topographic position, but FC and PWP would have been influenced by increased Silt % and Clay % at the lower DTW location. The soil moisture determinations MC1 and MC2 determinations for 11 July 1977 and 27 August 1977 were - in terms of dryness - closer to PWP than to FC, with some of the MC1 determination trending higher at low DTW levels. This was not the case for MC2 on 27 August 1977.

3.5. Regression Analyses: NO_3-N versus NH_4-N Retention

Figure 7 (right) reveals a significant trend towards increasing NO_3-N levels with decreasing DTW > 0.25 ha. This relationship becomes even more significant by noting that four of the five NO_3-N > 12 mg/g levels occurred close to the tracked-DTW > 0.25 ha flow paths in Figure 2. Adjusting the log_{10} (DTW > 0.25 ha) values for these points to 1 cm and deleting the remaining outlier modified the best-fitted regression result in Figure 7 (right) to become NO_3-N = 5.12 - 2.5 log_{10} (DTW > 0.25 ha); R^2 = 0.408. In contrast, the corresponding NH_4-N pattern remained low with no significant DTW trend.

3.6. Influences of Topography and Other Factors on the Surveyed Soil Properties

Factor analyzing the correlation matrix in Table 2 revealed three factors that account for 46.9% of the total correlation variance. The resulting polygonised factor-to-factor association pattern is presented in **Figure 8**, showing Factor 2 versus Factor 1 and Factor 3 versus Factor 2. The Factor that is not represented along the x- and y-axes appears as the polygon at or near the center. In terms of the total variance represented by the correlation matrix, F1 accounts for 26.0%, and can be interpreted as a Soil Loss Factor with its positive loadings for DTW, CF % and Sand % content, and its negative loadings for moisture (MC1 %) and Silt %. Factor 2 accounts for 11.6 % of the total variance and can be interpreted as a Soil Cropping factor, with its Mehlich-3 > 0.5 loadings referring to Ca, Mg, K, P, S, NO3-N, and Mn. Factor 3 accounts for 9.3% of the total variance and can be interpreted as a organo-metal complexation (SOM, or TOC) factor due to the polygon-represented loadings involving TOC, Ap, Fe, Zn, Cu, and Cs^{137} [10].

Note that there is an overall upland-to-downhill drift of the positive and negative F1 loadings for F2. This is likely due to persistent uphill-to-downhill transfer of water and soil sediments. Also note the positive Mn loading on Factor 2. This could be due to Mn applications intended to control common scab proliferations (*Streptomyces scabies*; [11]). The positive TOC-linked F2 entry for Cu could be due to foliar Cu applications intended to control occurrences of potato blight (*Phytophtora infestans*), scab and black-scurf inducing *Rhizoctania*, and potato-damaging nematodes ([12] [13]). Similarly, the TOC complexed Zn loading to F3 could be due to Zn applications intended to improve tuber yields [14]. The negative < - 0.25 F3 loadings for NO_3-N and NH_4-N in the F3 versus F2 plot of **Figure 8** reflect the tendency of soil organic matter to retain ions in the following order:

$$NO_3\text{-N} << NH_4\text{-N} < K \approx Na \approx Cs^{137} < Mg \approx Ca < Mn \approx Zn \approx Cu < Fe.$$

3.7. Multivariate Analysis

The multivariate analysis results in **Table 4** serve to elaborate on the Factor 1, 2, 3 patterns for the chemical soil properties in **Table 1** in quantitative terms, as follows.

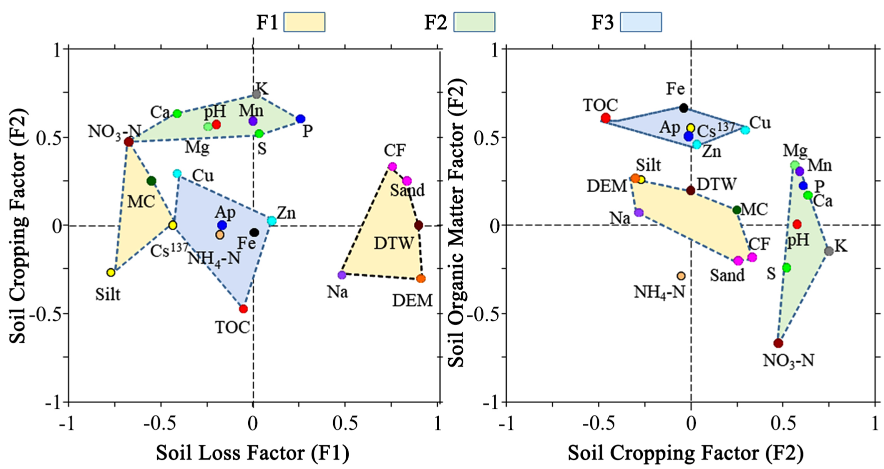

Figure 8. Factor analysis: Soil Cropping Factor (F2) versus Soil Loss factor (F1), left; Soil Organic Matter Factor (F3) versus Soil Cropping Factor (F2), right.

Table 4. Multivariate regression results for the soil chemical variables listed in Table 1.

	Dependent variable	Intercept		Variable 1		Variable 2		Variable 3		Variable 4		R^2	RMSE
		Coeff.	Std. Error	Coeff.	Std. Error	Coeff.	Std. Error	Coeff.	Std. Error	Coeff.	Std. Error		
Equation (1)	Mg	66.1	7.6	Ca								0.585	16.4
				0.081	0.005								
Equation (2)	Zn	1.14	0.3	Cu		DTW > 4 ha						0.232	0.701
				0.364	0.051	0.055	0.013						
Equation (3)	C	0.26	0.28	Silt		NO_3-N						0.274	0.225
				0.048	0.006	−0.040	0.007						
Equation (4)	P	−73.7	34.4	Ca		Mn		Sand %				0.535	36.5
				0.068	0.013	2.22	0.28	6.2	0.7				
Equation (5)	S	238	25	K		pH-H_2O		Ca				0.355	14.1
				0.224	0.027	−43.0	5.5	0.024	0.005				
Equation (6)	Mn	−35.1	4.6	Ca		Fe		P				0.523	7.73
				0.015	0.003	0.111	0.017	0.079	0.012				
Equation (7)	Ca	−1727	257	pH-H_2O		P		DTW > 4 ha				0.553	160
				513	49	1.76	0.23	−0.182	0.03				
Equation (8)	NO_3-N	−0.77	0.68	NH_4-N		DTW > 4 ha		K				0.585	1.61
				6.67	0.63	−0.323	0.029	0.029	0.003				
Equation (9)	pH-H_2O	4.6	0.1	Ca		S		K				0.554	0.165
				0.00058	0.00005	−0.0056	0.0007	0.0022	0.0003				
Equation (10)	NH_4-N	0.47	0.05	K		DTW > 4 ha		NO_3-N				0.42	0.149
				−0.0016	0.0003	0.020	0.003	0.042	0.004				
Equation (11)	Cu	0.449	0.07	Ca		Sand		Fe		P		0.630	0.055
				0.00014	0.00002	−0.0097	0.0013	0.00075	0.00002	0.00046	0.0001		
Equation (12)	Cs^{137}	−3884	474	Silt		K		C		Cu		0.546	332
				73.1	10.9	3.0	0.6	472	100	125	26		
Equation (13)	Fe	431	44	Cu		Mn		NO_3-N		pH-H_2O		0.421	26.6
				12.3	2.1	0.94	0.17	−4.1	0.8	−36.7	8.6		
Equation (14)	K	−109	51	pH		NO_3-N		P		NH_4-N		0.42	31.4
				38.9	9.6	7.1	1.0	0.24	0.04	−87.4	12.8		

1) Mehlich-3 extracted Mg is highly correlated with Ca (Equation (1)), possibly due to the presence of calcareous soil parent materials (e.g., the Carleton Forest Soil Association) and/or dolomitic Ca/Mg carbonate applications [15].

2) Mehlich-3 extracted Ca increases with soil pH and P but decreases with increasing DTW > 4 ha (Equation (7)). Part of this would be due to pH-elevating Ca carbonate applications. Also, the flow of water-soluble Ca would enrich extractable Ca and Mg at low DTW > 4 ha field locations.

3) The elevating Ca effect on pH effect can also be noted with Equations (4) and (9). In general, increasing the soil pH:

a) facilitates increases in P availability;

b) compensates for soil-acidifying Ca, Mg, K, and NH_4-N root uptake;

c) reduces the possibility of low-pH induced P fixation, and root-damaging Al (aluminum) and Mn mobilizations [16] [17].

4) Equations (5) and (9) reflect that S applications not only involve pH-neutral $CaSO_4$ (gypsum) and K_2SO_4 for adjusting S deficiencies, but also elemental S applications to enforce downward scab-eliminating pH adjustments [18] [19] [20].

5) Equations (8) and (10) suggest that increasing NO_3-N and NH_4-N levels would in part be due to NO_3-N and NH_4-N applications, possibly involving KNO_3, NO_3NH_4 and/or urea. **Figure 7** (right) indicates that NH_4-N content << NO_3-N content. This suggests that applying NH_4-N or urea as N fertilizer was likely not practiced due to NH_4-induced a) soil acidifying nitrification [21], b) greater potatoes tolerance for NO_3-N than for NH_4-N [22], and c) NH_4-N induced K displacement from soil cation exchange sites (Equation (10)). The slight NH_4-N increase with increasing DTW > 4 ha (Equation (10)) corresponds with lower denitrification rates on well-aerated upland field locations [23]. The more significant NO_3-N increase with decreasing DTW > 4 ha (**Figure 7**, right) would be due to uphill-to-downhill NO_3-N leaching from coarse-textured soils with low anion retention capacities [24].

6) As per Equations (8), (9), and (14), K increases with increasing NO_3-N but decreases with increasing NH_4-N. The former likely relates to KNO_3 and K phosphate applications, while the latter would be due to K-induced displacement of exchangeable NH_4-N. Altogether, Mehlich-3 extracted K is affected by four variables, namely pH, NO_3-N, P, and DTW > 4 ha (Equation (14)).

7) Mehlich-3 extracted P would not only increase by way of Ca phosphate applications [25], but is also seen to increase with increasing Mn and Sand % content (Equation (4)). The significant contributions of Mn to P (Equation (6)) could be due to Mn phosphate applications. The decrease in extractable P with decreasing Sand % could be due to lower P-fixing Fe content along the lower areas of the field [26] [27].

8) Mehlich-3 extracted Cu, Fe, Mn, Zn, Cs^{137} are linked to one another via Factor 3, but their quantitative dependencies are element specific. In detail:

a) Mehlich-3 extracted Zn is primarily related to Mehlich-3 extractable Cu but weakly so with increasing DTW > 4 ha (Equation (2)).

b) Mehlich-3 extracted Mn and Cu are in part quantified by Mehlich-3 extractable Fe (Equations (6) and (11)), with Cu also increasing with increasing Ca, P, and Sand % content.

c) Mehlich-3 extracted Cs^{137} increases with Mehlich-3 extracted Cu, soil C, plough player depth and Silt % (Equation (12)). Hence, soil C and Mehlich-3 extracted Cs^{137} increase slightly from the upland to the lowland field locations.

The Mehlich-3 extracted Cu, Zn and Cs^{137} fractions are also indirectly related to increasing DTW 4 > ha in a positive or negative sense, *i.e.*, positive for Zn (+) via the positive relationship between Zn and DTW (Equation (2)), negative for Cs^{137} via decreasing Silt % with increasing DTW (**Figure 4**), and negative for Cu via increasing Sand % with increasing DTW (**Figure 4**).

9) Mehlich-3 extracted Fe increased with increasing Mehlich-3 extracted Cu and Mn but decreased with increasing NO_3-N and pH (Equation (13); [28]. In general, increasing pH leads to decreased Fe hydroxide solubility. Decreased Fe extractability with increasing NO_3-N in low-lying and less aerobic field locations would therefore be due to loss of redox-solubilized Fe.

10) While Cs^{137} is associated with TOC (+), K (+), Cu (+), and Silt % (+) according to Equation (12) in **Table 4** ($R^2 = 0.546$), it is also higher at low DTW locations, *i.e.*,

$CS^{137} = 1641 - 291 \log_{10} (DTW > 0.25 \text{ ha})$; $R^2 = 0.111$.

In contrast, TOC does not vary significantly with DTW, *i.e.*,

$TOC = 2.23 - 0.009 (DTW > 1 \text{ ha})$; $R^2 = 0.010$.

The CS^{137} vs. DTW trend therefore contrasts the lack of a TOC vs. DTW trend. This difference is likely due to observations that Cs^{137} binds more strongly to mineral surfaces than to organic matter [29]. Hence, the downhill CS^{137} trend is likely due to erosion-induced uphill-downhill silt transfer **Figure 9**, [30].

11) According to **Table 2** correlations, TOC increased with increasing Silt, Clay, NO_3-N and NH_4-N content but decreased with increasing Sand and CF content. Among these, the increase with Silt % and the decrease with NO_3-N are more significantly related to TOC (Equation (3)). Generally, TOC increases downhill in silt-accumulating depressions across hummocky fields [30] [31] [32] [33], but - in this survey - uphill to downhill TOC did not vary significantly (**Figure 10**), *i.e.*,

$TOC \% = 2.20 - 0.018 \log_{10} (DTW > 0.25 \text{ ha})$; $R^2 = 0.002$ and

$TOC \% = 2.00 + 0.0039 \text{ DEM}$; $R^2 = 0.0018$.

In part, this could be due that TOC % remains low due to increased downhill Silt % and Clay %. To that effect, TOC only varies from 1.4% to 3% while Silt and Clay increase from uphill to downhill by about 6 and 3%, respectively (**Figure 4**).

12) The effect of topography on in-field soil property variations was further detailed by [34] based on 774 survey points spread across New Brunswick. That study summarized the trends so observed in terms of three topographically re-

lated Factors, as follows:

a) The dominant Factor referred to the increasing Sand (+), CF (+) and Soil Organic Carbon (SOC, +) in association with decreasing Silt (−), Labile N (−) and Particulate Organic Carbon (POC, −). These trends are similar to the above results, except that SOC (≈4 POC) should be increasing with increasing Silt %, as is the case for this study (Table 2, Equation (3), Figure 10).

b) The second Factor refers to the uphill decreasing effects on pH (−) and labile N (−), as is the case in Table 2 with respect to pH and NO_3-N.

c) The third Factor refers to an increasing effect of curvature on soil resistance to penetration (+), and CF % (+). Based on curvature across eroding knolls, CF % (+) can be expected to vary with Sand % (+), Silt % (−) and DTW (+). Adding curvature as independent variable to the analysis of the 1977 survey results did not affect the results reported above.

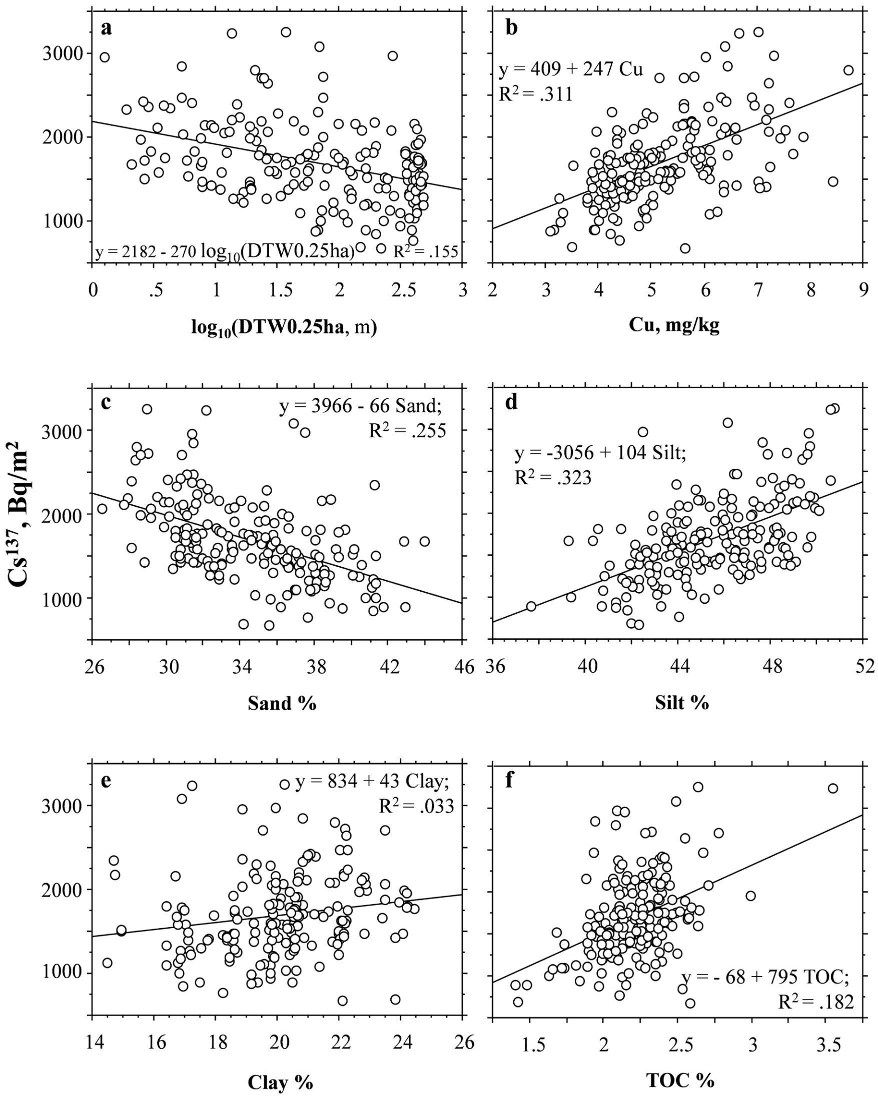

Figure 9. Scatterplots of Cs^{137} versus (a): $\log_{10}$ (DTW > 0.25ha, m); (b): Cu; (c): Sand; (d): Silt; (e): Clay; (f): TOC.

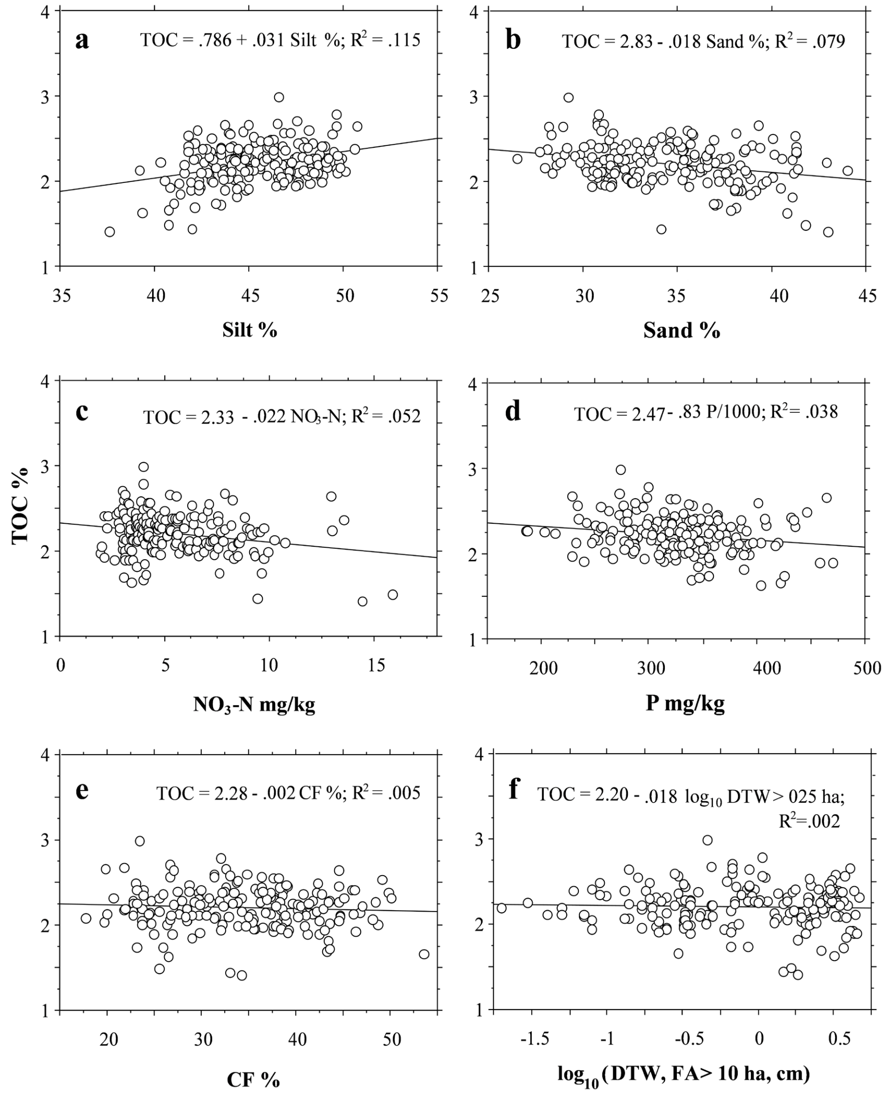

Figure 10. Scatterplots of TOC % versus (a): Silt %; (b): Sand %; (c): NO_3-N; (d): P; (e): CF %; and (f): $\log_{10}$ (DTW > 0.25 ha).

4. Conclusions

In summary, it is now possible to quantify erosion- and water-flow induced changes in elevations and surveyed soil properties across fields, at high-resolution. In detail, the regression results in Table 3 suggest that the point-generated elevations were somewhat smoother in 1997 than in 2017. This change was likely due to continuing soil erosion, which would further expose upslope rocks and other coarse fragments and lowering up-field soil organic matter while deepening silt-enriched flow channels in the downslope locations.

Factor analyzing the variables in Table 1 revealed three variation-controlling factors. Factor 1 links the uphill-to-downhill pattern for sand, silt, clay, and CF to the cartographic DTW index. Factor 2 refers to periodic N, Ca, Mg, K, S, Mn and P soil amendments, while Factor 3 reflects the retention of heavy metals such Fe, Zn, Cu and Cs^{137} by SOM (or TOC), and includes increased NO_3-N levels in low-lying areas due to low SOM anion retention.

The variables that are directly or indirectly affected by DTW refer to:

1) Sand %, Silt %. Clay % and CF %; these increased with increasing DTW > 4 ha;

2) MC1, FC, PWP; these increased with decreasing DTW > 0.25 ha;

3) NO_3-N, Ca, Mg, Cu, Cs^{237}; these decreased with increasing $\log_{10}$ (DTW > 0.25 ha) pattern.

The cumulative effects of soil erosion and retention manifest themselves at the DTW > 4 ha scale. In contrast, the cumulative effects of water flow and retention manifest themselves at the DTW > 0.25 ha and $\log_{10}$ (DTW > 0.25 ha) scales, with the former and latter pertaining to soil moisture content and Mehlich-3 element concentrations, respectively. In contrast, TOC % was not related to DTW in this study, but the reported uphill-to-downhill TOC % variations [30] [32] [33] likely vary at the DTW > 4 ha scale as well.

In the absence of locally repeated field surveys, one-time soil property assessments such as above do not lend themselves for quantifying cause-and-effect relationships related to sequential crop management actions. Nevertheless, the analytical results and related correlations so derived are consistent with 1) quantifying topo-induced soil property changes and 2) potato-cropping recommendations with respect to regular and/or intermittent N, P, K, Ca, Mg, S, Fe, Mn, B, Cu, and Zn applications as summarized (see, e.g., [35]).

Acknowledgments

The preceding work is based on the Agriculture and Agri-food Canada field survey data centered on the Hartland potato field, with many thanks to Lien Chow for making these data available. Also much appreciated is the free GeoNB registered access to the 1-m resolution LiDAR DEM for New Brunswick, and financial assistance received from the New Brunswick Agriculture Department for crop suitability mapping.

Conflicts of Interest

The authors declare no conflicts of interest regarding the publication of this paper.

References

[1] Zebarth, B.J., Rees, H., Walsh, J., Chow, L. and Pennock, D.J. (2002) Soil Variation within a Hummocky Podzolic Landscape under Intensive Potato Production. *Geoderma*, **110**, 19-33. https://doi.org/10.1016/S0016-7061(02)00213-6

[2] GeoNB (2019) Lidar Data. http://www.snb.ca/geonb1/e/DC/lidarData.asp

[3] Murphy, P.N.C., Ogilvie, J. and Arp, P.A. (2009) Topographic Modelling of Soil Moisture Conditions: A Comparison and Verification of Two Models. *European Journal of Soil Science*, **60**, 94-109. https://doi.org/10.1111/j.1365-2389.2008.01094.x

[4] White, B., Ogilvie, J., Campbell, D.M.H., Hiltz, D., Gauthier, B., Chisholm, H., Wen, K.H., Murphy, P.N.C. and Arp, P.A. (2012) Using the Cartographic Depth-to-

Water Index to Locate Small Streams and Associated Wet Areas across Landscapes. *Canadian Water Resources Journal*, **37**, 333-347. https://doi.org/10.4296/cwrj2011-909

[5] Shiwakoti, S., Zheljazkov, V.D., Gollany, H.T., Kleber, M. and Xing, B. (2019) Micronutrients Decline under Long-Term Tillage and Nitrogen Fertilization. *Scientific Reports*, **9**, Article No. 12020. https://doi.org/10.1038/s41598-019-48408-6

[6] Tarboton, D.G. (1997) A New Method for the Determination of Flow Directions and Upslope Areas in Grid Digital Elevation Models. *Water Resources Research*, **33**, 309-319. https://doi.org/10.1029/96WR03137

[7] Guisan, A., Weiss, S.B. and Weiss, A.D. (1999) GLM versus CCA Spatial Modeling of Plant Species Distribution. *Plant Ecology*, **143**, 107-122. https://doi.org/10.1023/A:1009841519580

[8] Weiss, A.D. (2001) Topographic Position and Landforms Analysis. *Poster Presentation*, *ESRI User Conference*, San Diego, 9-13 July 2001.

[9] Balland, V., Pollacco, J.A.P. and Arp, P.A. (2008) Modeling Soil Hydraulic Properties for a Wide Range of Soil Conditions. *Ecological Modelling*, **219**, 300-316. https://doi.org/10.1016/j.ecolmodel.2008.07.009

[10] Baken, S., Degryse, F., Verheyen, L., Merckx, R. and Smolders, E. (2011) Metal Complexation Properties of Freshwater Dissolved Organic Matter Are Explained by Its Aromaticity and by Anthropogenic Ligands. *Environmental Science & Technology*, **45**, 2584-2590. https://doi.org/10.1021/es103532a

[11] McGregor, A.J. and Wilson, G.C.S. (1966) The Influence of Manganese on the Development of Potato Scab. *Plant and Soil*, **25**, 3-16. https://doi.org/10.1007/BF01347957

[12] Finckh, M.R., Schulte-Geldermann, E. and Bruns, C. (2006) Challenges to Organic Potato Farming: Disease and Nutrient Management. *Potato Research*, **49**, 27-42. https://doi.org/10.1007/s11540-006-9004-3

[13] Dhaliwal, S.S., Naresh, R.K., Mandal, A., Singh, R. and Dhaliwal, M.K. (2019) Dynamics and Transformations of Micronutrients in Agricultural Soils as Influenced by Organic Matter Build-up: A Review. *Environmental and Sustainability Indicators*, **1-2**, Article ID: 100007. https://doi.org/10.1016/j.indic.2019.100007

[14] White, P.J., Broadley, M.R., Hammond, J.P., Ramsay, G., Subramanian, N.K., Thompson, J. and Wright, G. (2012) Bio-Fortification of Potato Tubers Using Foliar Zinc-Fertiliser. *The Journal of Horticultural Science and Biotechnology*, **87**, 123-129. https://doi.org/10.1080/14620316.2012.11512842

[15] Kostic, L., Nikolic, N., Samardzic, J., *et al.* (2015) Liming of Anthropogenically Acidified Soil Promotes Phosphorus Acquisition in the Rhizosphere of Wheat. *Biology and Fertility of Soils*, **51**, 289-298. https://doi.org/10.1007/s00374-014-0975-y

[16] Ondrasek, G., Kranjčec, F., Filipović, L., Filipović, V., Bubalo Kovačić, M., Badovinac, I. J., Peter, R., Petravić, M., Macan, J. and Rengel, Z. (2021) Biomass Bottom Ash & Dolomite Similarly Ameliorate an Acidic Low-Nutrient Soil, Improve Phytonutrition and Growth, but Increase Cd Accumulation in Radish. *Science of the Total Environment*, **753**, Article ID: 141902. https://doi.org/10.1016/j.scitotenv.2020.141902

[17] Holmström, S.J.M., Van Hees, P.A.W. and Lundström, U.S. (2005) Modelling of Aluminium Chemistry in Soil Solution of Untreated and Dolomite Treated Podzolic Soil. *Geoderma*, **127**, 280-292. https://doi.org/10.1016/j.geoderma.2004.12.012

[18] Klikocka, H., Haneklaus, S., Bloem, E. and Schnug, E. (2005) Influence of Sulfur Fertilization on Infection of Potato Tubers with *Rhizoctonia solani* and *Strepto-*

myces scabies. *Journal of Plant Nutrition*, **28**, 819-833. https://doi.org/10.1081/PLN-200055547

[19] Haddad, M., Bani Hani, N., Al-Tabbal, J. and Al-Fraihat, A. (2016) Effect of Different Potassium Nitrate Levels on Yield and Quality of Potato Tubers. *Journal of Food, Agriculture & Environment*, **14**, 101-107.

[20] Penn, C.J., Rutter, E.B., Arnall, D.B., Camberato, J., Williams, M. and Watkins, P.A. (2018) Discussion on Mehlich-3 Phosphorus Extraction from the Perspective of Governing Chemical Reactions and Phases: Impact of Soil pH. *Agriculture*, **8**, Article No. 106. https://doi.org/10.3390/agriculture8070106

[21] Hagin, J., Olsen, S.R. and Shaviv, A. (1990) Review of Interaction of Ammonium-Nitrate and Potassium Nutrition of Crops. *Journal of Plant Nutrition*, **13**, 1211-1226. https://doi.org/10.1080/01904169009364147

[22] Cao, W. and Tibbitts, T.W. (1998) Response of Potatoes to Nitrogen Concentrations Differs with Nitrogen Forms. *Journal of Plant Nutrition*, **21**, 615-623. https://doi.org/10.1080/01904169809365429

[23] Kelling, K.A., Wolkowski, R.P. and Ruark, M.D. (2011) Potato Response to Nitrogen Form and Nitrification Inhibitors. *American Journal of Potato Research*, **88**, 459-469. https://doi.org/10.1007/s12230-011-9212-5

[24] Shrestha, R.K, Cooperband, L.R. and MacGuidwin, A.E. (2010) Strategies to Reduce Nitrate Leaching into Groundwater in Potato Grown in Sandy Soils: Case Study from North Central USA. *American Journal of Potato Research*, **87**, 229-244. https://doi.org/10.1007/s12230-010-9131-x

[25] Hopkins, B.G., Horneck, D.A. and MacGuidwin, A.E. (2014) Improving Phosphorus Use Efficiency through Potato Rhizosphere Modification and Extension. *American Journal of Potato Research*, **91**, 161-174. https://doi.org/10.1007/s12230-014-9370-3

[26] Fixen, P.E. and Bruulsema, T.W. (2014) Potato Management Challenges Created by Phosphorus Chemistry and Plant Roots. *American Journal of Potato Research*, **91**, 121-131. https://doi.org/10.1007/s12230-014-9374-z

[27] Mansfeldt, T. (2004) Redox Potential of Bulk Soil and Soil Solution Concentration of Nitrate, Manganese, Iron, and Sulfate in Two Gleysols. *Journal of Plant Nutrition and Soil Science*, **167**, 7-16. https://doi.org/10.1002/jpln.200321204

[28] Schwab, A.P. (1989) Manganese-Phosphate Solubility Relationships in an Acid Soil. *Soil Science Society of America Journal*, **53**, 1654-1660. https://doi.org/10.2136/sssaj1989.03615995005300060007x

[29] Andersson, K.G. and Roed, J. (1994) The Behaviour of Chernobyl ^{137}Cs, ^{134}Cs and $^{m°6}Ru$ in Undisturbed Soil: Implications for External Radiation. *Journal of Environmental Radioactivity*, **22**, 183-196. https://doi.org/10.1016/0265-931X(94)90080-9

[30] Ritchie, J.C., McCarty, G.W., Venteris, E.R. and Kaspar, T.C. (2007) Soil and Soil Organic Carbon Redistribution on the Landscape. *Geomorphology*, **89**, 163-171. https://doi.org/10.1016/j.geomorph.2006.07.021

[31] Kaspar, T.C., Pulido, D.J., Fenton, T.E., Colvin, T.S., Karlen, D.L. Jaynes, D.B. and Meek, D.W. (2004) Relationship of Corn and Soybean Yield to Soil and Terrain Properties. *Agronomy Journal*, **96**, 700-709. https://doi.org/10.2134/agronj2004.0700

[32] Wehrhan, M. and Sommer, M. (2021) A Parsimonious Approach to Estimate Soil Organic Carbon Applying Unmanned Aerial System (UAS) Multispectral Imagery and the Topographic Position Index in a Heterogeneous Soil Landscape. *Remote Sensing*, **13**, Article No. 3557. https://doi.org/10.3390/rs13183557

[33] Driscoll, B.A., Krzica, M., Comeau, L.-P., Eskelson, B.N.I. and Li, S. (2023) Short-Term Response of Soil Aggregate Stability and Labile Carbon to Contour Tillage, Diversion Terrace, Grassed Waterway, and Tile Drainage Implementation. *Canadian Journal of Soil Science*. https://doi.org/10.1139/cjss-2022-0094

[34] Zebarth, B.J., Moreau, G., Dixon, T., Fillmore, S., Smith, A., Hann, S. and Comeau, L.-P. (2022) Soil Properties and Topographic Features Influence within-Field Variation in Potato Tuber Yield in New Brunswick, Canada. *Soil Science Society of America Journal*, **86**, 134-145. https://doi.org/10.1002/saj2.20342

[35] Government of New Brunswick (2022) Soil Management. https://www2.gnb.ca/content/gnb/en/departments/10/agriculture/content/crops/potatoes/soil_management.html